0888-8809/06/$15.00/0
Printed in U.S.A.

Molecular Endocrinology 20(1):183–193

doi: 10.1210/me.2005-0157

Syntaxin 4 Facilitates Biphasic Glucose-Stimulated Insulin Secretion from Pancreatic β-Cells

Beth A. Spurlin and Debbie C. Thurmond

Department of Biochemistry & Molecular Biology, Center for Diabetes Research, Indiana University School of Medicine, Indianapolis, Indiana 46202

Numerous overexpression studies have recently implicated Syntaxin 4 as an effector of insulin secretion, although its requirement in insulin granule exocytosis is unknown. To address this, islets from Syntaxin 4 heterozygous (−/+) knockout mice were isolated and compared with islets from wild-type mice. Under static incubation conditions, Syntaxin 4 (−/+) islets showed a 60% reduction in glucose-stimulated insulin secretion compared with wild-type islets. Perifusion analyses revealed that Syntaxin 4 (−/+) islets secreted 50% less insulin during the first phase of glucose-stimulated insulin secretion and that this defect could be fully restored by the specific replenishment of recombinant Syntaxin 4. This essential role for Syntaxin 4 in secretion from the islet was localized to the β-cells because small interfering RNA-mediated depletion of Syntaxin 4 in MIN6 β-cells abolished glucose-stimulated insulin secretion. Moreover, immunofluorescent confocal microscopy revealed that Syntaxin 4 was principally localized to the β-cells and not the α-cells of the mouse islet. Remarkably, islets isolated from transgenic mice that express 2.4-fold higher levels of Syntaxin 4 relative to wild-type mice secreted approximately 35% more insulin during both phases of insulin secretion, suggesting that increased Syntaxin 4 may be beneficial for enhancing biphasic insulin secretion in a regulated manner. Taken together, these data support the notion that Syntaxin 4-based SNARE complexes are essential for biphasic insulin granule fusion in pancreatic β-cells. (*Molecular Endocrinology* 20: 183–193, 2006)

THE PANCREATIC β-cell responds to increases in circulating glucose levels by releasing insulin in a highly regulated manner. Initiation of the process occurs when glucose enters the cell through the glucose transporter (GLUT2) present on the plasma membrane, which is rapidly metabolized, causing an increase in the cellular ATP/ADP ratio. In response to the altered ATP/ADP ratio the K_{ATP}-sensitive channels close and evoke membrane depolarization, which leads to activation of the L_{type}-voltage-dependent calcium channels. The resultant increase in intracellular calcium triggers first phase insulin release (1–5). First-phase secretion is attributed to the fusion and release of insulin from granules clustered at the cell surface, termed the ready releasable pool, whereas second phase entails the mobilization and trafficking of intracellular storage pools of insulin secretory granules to the plasma membrane (6, 7). Whereas the mechanism has not been fully elucidated, fusion of insulin secretory granules is known to be regulated by soluble N-ethylmaleimide sensitive factor attachment protein receptor (SNARE) protein complexes at the plasma membrane.

Upon stimulation with glucose, the target membrane t-SNARE proteins Syntaxin 1 (Syn1) and SNAP-25 [soluble NSF (N-ethylmaleimide sensitive factor) attachment protein] receptor tether the insulin granules to the plasma membrane through interaction with their cognate vesicle v-SNARE protein, vesicle-associated membrane protein VAMP2. These three proteins form a heterotrimeric SNARE core complex, which through an undefined mechanism facilitates the fusion of the insulin secretory granule with the plasma membrane and release of insulin from the cell (8–11). Insulin secretion is known to be mediated by a VAMP2-dependent mechanism because cleavage of VAMP2 abolishes all insulin secretion (11, 12). Cleavage of SNAP-25 only reduces insulin secretion by 50% (8) but can be substituted for by the abundant SNAP-23 isoform in Syn1-based SNARE complexes. However, inactivation of Syn1 reduces glucose-stimulated insulin secretion only by 25% (12, 13), suggesting that another Syntaxin isoform might be responsible for the remainder of VAMP2-dependent glucose-stimulated insulin secretion.

In fact, islet β-cells express detectable levels of three additional plasma membrane-localized Syntaxin isoforms, Syntaxins 2, 3, and 4 (9, 14–16). Recent studies have indirectly implicated the Syntaxin 4

First Published Online August 11, 2005

Abbreviations: CHO, Chinese hamster ovary; Con-Ad, control adenovirus; EGFP, enhanced green fluorescent protein; FITC, fluorescein isothiocyanate; GLUT, glucose transporter; M.O.I., multiplicity of infection; nt, nucleotides; siCon, control siRNA sequence; siRNA, small interfering RNA; SNAP, [soluble NSF (N-ethylmaleimide sensitive factor) attachment protein] receptor; Syn4 Tg, Syntaxin 4 transgenic; t-SNARE, target SNARE; v-SNARE, vesicle SNARE.

***Molecular Endocrinology* is published monthly by The Endocrine Society (http://www.endo-society.org), the foremost professional society serving the endocrine community.**

(Syn4) isoform in insulin granule exocytosis, in that multiple Syn4 binding proteins participate in glucose-stimulated insulin secretion (17–19). Syn4 is best characterized as the t-SNARE which facilitates glucose uptake into skeletal muscle and adipose tissue (20–27). We have previously shown that Munc18c, the high-affinity binding partner to Syn4, was essential for normal glucose-stimulated insulin secretion in mouse islets (17). Furthermore, sequestration of Syn4 by overexpression of the Syn4-interacting protein synip resulted in inhibited insulin secretion and inhibition of the interaction between Syn4 and VAMP2 in insulin-secreting βHC-9 cells (18). Whereas these data provide indirect support for a functional role for Syn4 in exocytosis of insulin secretory granules from the pancreatic β-cell, it is unclear as to whether it is essential to the process.

In the present study, we provide the first direct evidence for a positive and essential role for Syn4 in regulating biphasic glucose-stimulated insulin secretion. Islets isolated from Syn4 (−/+) heterozygous knockout mice displayed a significant 50% reduction in the first phase of glucose-stimulated insulin secretion, and this deficit was normalized by adenoviral-mediated restoration of Syn4 protein levels. Syn4 was visualized principally in the β- and not the α-cells of the islet, suggesting that its role was in the insulin-secreting β-cells. Consistent with data generated from Syn4 (−/+) islets, reduced glucose-stimulated insulin secretion was recapitulated using Syn4-specific small interfering RNA (siRNA)-mediated knockdown in MIN6 cells. Remarkably, islets isolated from transgenic mice that overexpress Syn4 protein showed significantly enhanced biphasic insulin secretion that was independent of alterations in insulin content. Taken together, these data suggest that increased Syn4 may be therapeutically beneficial and represent a new target for enhancing insulin release in a biphasic and regulatable manner.

RESULTS

Syntaxin 4 Is Required for Glucose-Stimulated Insulin Secretion from Islets

To determine the functional requirement for Syn4 in insulin secretion, islets were isolated from Syn4 heterozygous (−/+) knockout and wild-type mice. Analysis of protein abundances in the islets showed that Syn4 and Munc18c protein levels were specifically reduced by 40–50% in Syn4 (−/+) islets as compared with wild-type islets (Fig. 1, A and B). This coordinate reduction in Munc18c with alterations in Syn4 abundance is consistent with our previous observations in pancreas tissue extracts from Syn4 (−/+) mice (27). Also similar to our previous report, abundances of other Syn4 binding proteins and alternate SNARE isoforms such as Syn1, SNAP-25, and VAMP2 and were unchanged (Fig. 1, A and B). Functionally, wild-type islets showed a 19-fold increase in insulin secretion

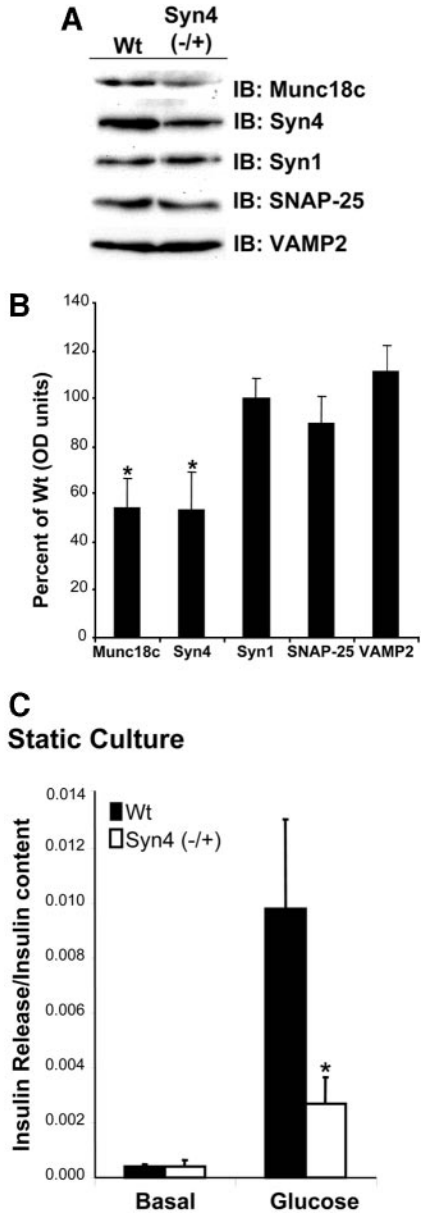

Fig. 1. Islets Isolated from Syn4 (−/+) Mice Have Impaired Glucose-Stimulated Insulin Secretion

Islets were isolated from wild-type (Wt) and Syn4 heterozygous (−/+) knockout mice as described in *Materials and Methods*. A, Approximately 200 islets isolated from each mouse strain were solubilized in SDS-sample buffer and resolved on 12% SDS-PAGE, transferred to polyvinylidene difluoride and immunoblotted (IB). B, OD scanning quantitation of three independent islet immunoblot experiments. Band density for Wt was set to 100% and data tabulated as the percentage of band density for Syn4 (−/+) relative to that of Wt, and are shown as means ± SE, *, $P < 0.05$ *vs.* Wt. C, Isolated islets were preincubated for 2 h in low glucose (2.8 mM) KRBH followed by a 2-h glucose stimulation (20 mM). Insulin released into the KRBH and insulin content of the islets was quantitated by RIA. Insulin released was normalized to insulin content performed in triplicate in each of three independent islet isolation experiments, and data are shown as the average ± SE; *, $P < 0.05$, wild-type glucose-stimulated secretion *vs.* Syn4 (−/+) stimulated secretion.

after a 2-h static incubation with 20 mM glucose, as we have reported previously (19), and Syn4 (−/+) islets secreted only 6-fold over basal (Fig. 1C). Wild-type and Syn4 (−/+) islets released similar levels of insulin under basal conditions (2.8 mM glucose), and the total insulin content did not differ. Thus, the reduction of Syn4 and Munc18c proteins in islets correlated with a significant decrease in glucose-stimulated insulin secretion.

The pancreatic islet is composed of multiple cell types, 70–80% of which are β-cells. To determine the relative abundance of Syn4 in the insulin-secreting β-cells of the islet, we used immunofluorescent confocal microscopy. Immunofluorescent labeling of wild-type mouse islets demonstrated that Syn4 colocalized with insulin secreting β-cells (Fig. 2A, panels 1–3), as evidenced by a high incidence of yellow signal in the merged image. By contrast, Syn4 did not appear to colocalize with the glucagon-secreting α-cells present at the perimeter of the mouse islet (Fig. 2A, panels 4–6). Moreover, to clearly visualize the plasma membrane localization of Syn4 in β-cells, MIN6 cultured β-cells were immunostained for Syn4 (Fig. 2A, panel 7). Immunostaining demonstrated the plasma membrane localization of Syn4, which showed a similar localization to the cell perimeter as the well-characterized β-cell t-SNARE protein SNAP-25 (Fig. 2A, panels 7 and 8). Furthermore, both Syn4 and SNAP-25 showed a lesser amount of intracellular punctuate labeling, which has also been reported in other cell types and thought to represent SNARE protein biogenesis and trafficking to the plasma membrane compartment (28). To biochemically confirm the plasma membrane localization of Syn4 in β-cells, MIN6 cells were subfractionated as described previously into three main compartments: granule, cytosol (soluble), and plasma membrane (29). The plasma membrane compartment was assessed for enrichment of the well-described Syn1 protein (30), the granule compartment was marked by the enrichment of phogrin (31) and VAMP2 (32), and the cytosolic fraction validated by the presence of soluble forms of Cdc42 (33) and Munc18c (34). Similar to the partitioning of Syn1, Syn4 abundance was highest in plasma membrane with a small amount present in the granule fraction and none in the cytosolic (soluble) fraction (Fig. 2B). These studies demonstrated that Syn4 was expressed and localized to the plasma membrane of insulin-secreting β-cells of the islet.

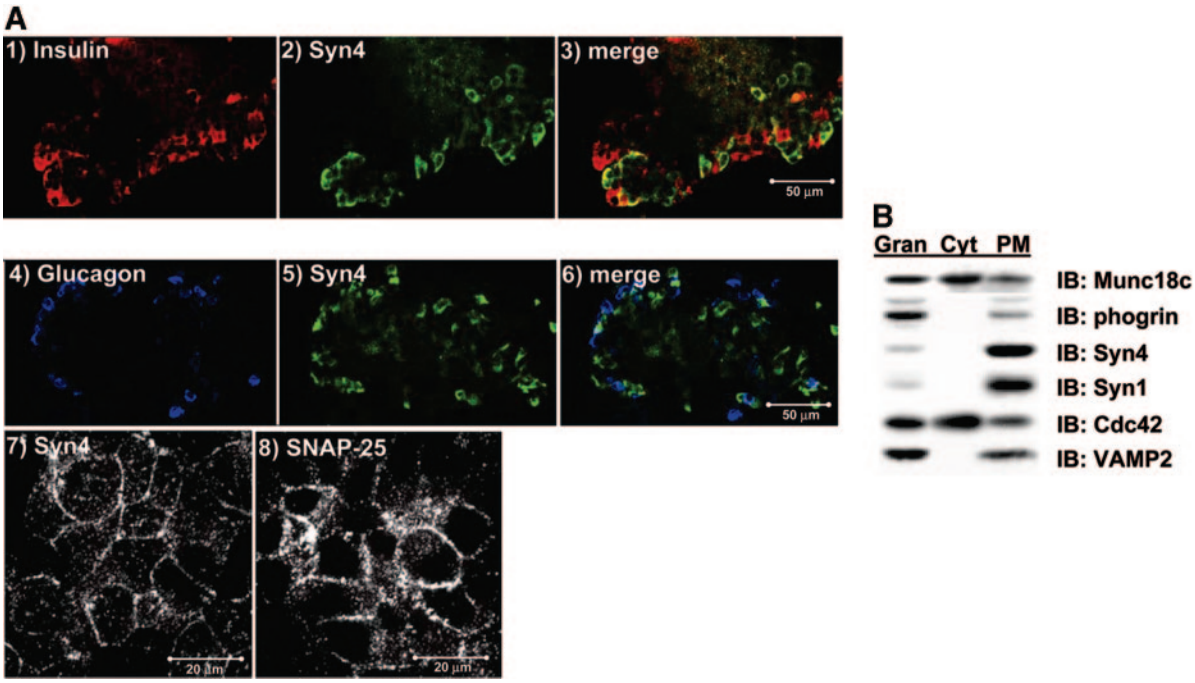

Fig. 2. Syn4 Protein Localizes to the Plasma Membrane of Insulin-Secreting β-Cells

A, Islets isolated from wild-type mice were fixed and permeabilized for immunostaining with mouse antiinsulin (panel 1), rabbit anti-Syn4 (panels 2 and 5) or guinea pig antiglucagon (panel 4) primary antibodies. Islets were fluorescently labeled by the addition of antimouse Texas Red, antirabbit FITC or antiguinea pig Cy5-conjugated secondary antibodies for visualization by confocal microscopy at the mid plane of islet cluster (×100 objective). Colocalization (*yellow*) is seen in merged images of Syn4 with insulin (panel 3). Merge of Syn4 with glucagon (panel 6) shows little to no colocalization (*white*). Immunofluorescent localization of Syn4 to the plasma membrane was performed in MIN6 β-cells using rabbit anti-Syn4 or mouse anti-SNAP-25 primary antibodies and Texas-Red secondary antibody (panels 7 and 8), and images captured with a ×100 objective (×3 zoom). All images are representative of greater than five independent fields. B, Subcellular fractionation of MIN6 cells and localization of exocytic proteins. MIN6 cells were incubated in glucose-free MKRBB for 2 h followed by fractionation. Fractions (30 μg granule and plasma membrane, 60 μg cytosolic protein per lane) were resolved on 12% SDS-PAGE and transferred to polyvinylidene difluoride for immunoblotting. Data are representative of three to five sets of fractions.

Depletion of Syntaxin 4 in MIN6 β-Cells Reduces Insulin Release

Unlike Syn1, Syn4 is not susceptible to cleavage by botulinum toxins (15, 35). Thus, to determine the potential involvement of Syn4 in insulin secretion, we used siRNA-mediated depletion of Syn4. Four different siRNA constructs were initially generated against Syn4 and introduced into Chinese hamster ovary (CHO)-K1 cells using a plasmid delivery system (pSilencer1.0; Ambion, Austin, TX). Because CHO-K1 cells express very low levels of endogenous Syn4 protein, cells were coelectroporated with recombinant Syn4 DNA plus one of the four different siRNA constructs to examine the capability of each siRNA to specifically deplete recombinant Syn4 expression. A control siRNA sequence (siCon) reported to lack recognition of mammalian sequences was included in each experiment (36). Cell lysates were prepared and assessed for Syn4 expression by immunoblotting (Fig. 3A). Quantitation of multiple sets of lysates using OD scanning showed that although all four siRNAs resulted in diminished levels of Syn4 to varying degrees, siRNA construct no. 3 exhibited the greatest reduction (80–85%). Given that the transfection efficiency as gauged by GFP fluorescence in electroporated cells was between 70% and 90% in each CHO-K1 electroporation, this level of knockdown suggested that the siRNA was at least 90% effective at targeting Syn4.

To determine whether the knockdown of Syn4 would alter basal or glucose-stimulated insulin secretion, we cotransfected MIN6 β-cells with the Syn4 siRNA with human proinsulin DNA and quantitated the release of human C-peptide. Human C-peptide, cleaved from human proinsulin, is immunologically distinct from the mouse C-peptide secreted from the MIN6 β-cells and therefore allows detection of insulin release specifically from transfected cells (37, 38). Transient transfection was performed using Tfx-50 reagent and achieved expression of recombinant protein in approximately 10–20% of the cell population. Similar to previous reports using this assay, glucose stimulated approximately 30% more human C-peptide compared with basal levels (37, 39, 40) in cells transfected with a control vector (pcDNA3) or siCon. By contrast, transfection of MIN6 cells with Syn4 siRNA abolished glucose-stimulated insulin secretion compared with the cells transfected with the control siRNA, but had no effect upon basal level secretion (Fig. 3B). Because of the low efficiency of transient transfection in the MIN6 cells we could not detect siRNA knockdown of Syn4; however, the functional ablation of glucose-stimulated human C-peptide release in consistent with the idea that Syn4 is essential for glucose-stimulated insulin secretion from β-cells.

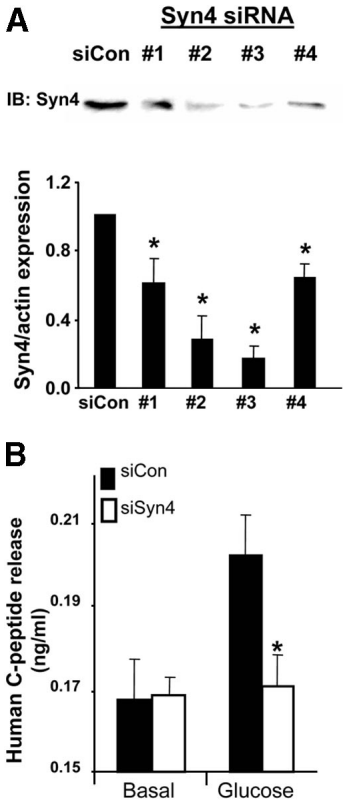

Fig. 3. siRNA-Mediated Knockdown of Syn4 Abolishes Glucose-Stimulated Insulin Secretion in MIN6 Cells

Four Syn4 siRNA double-stranded oligonucleotides were subcloned into the pSilencerU6–1.0 vector (Ambion). A, CHO-K1 cells were coelectroporated with siRNA constructs and pcDNA3-Syn4 as a reporter of knockdown (CHO-K1 cells have very low levels of endogenous Syn4 protein). After 48 h incubation, detergent lysates were prepared and subjected to 10% SDS-PAGE for immunoblotting with anti-Syn4 and antiactin (loading control) antibodies. B, MIN6 cells were cotransfected using Tfx-50 (Promega) with either control or Syn4 siRNA plasmid DNAs (siCon and siSyn4, respectively) plus human proinsulin DNA as described *in Materials and Methods*. After 48 h incubation, cells were incubated in glucose-free or 20 mM glucose in MKRBB for 60 min. Human C-peptide derived from the transfected cells and secreted into the media was measured by RIA. Data represent the average ± SE for four independent CHO-K1 electroporation and MIN6 transfection experiments with at least two independent batches of cesium chloride-purified DNA. *, $P < 0.05$, *vs.* siCon.

Syntaxin 4 Functions in First-Phase Insulin Secretion

Although there was diminished glucose-stimulated insulin secretion from Syn4 (−/+) islets during static culture, the constraints of the static incubation experiment fail to distinguish whether Syn4 mediates first, second ,or both phases of glucose-stimulated insulin secretion. Therefore, to determine which phase of glucose-stimulated insulin secretion required Syn4, we perifused islets isolated from Syn4 (−/+) or wild-type

mice in parallel chambers and measured insulin secretion every min over a 60-min time period (Fig. 4A). After an equilibration period of 30 min, islets were perifused for 10 min in KRBH buffer containing 2.8 mM glucose (basal), followed by stimulation for 35 min at 20 mM glucose, and finally returned to basal conditions for an additional 15 min. Insulin release kinetics showed biphasic responsiveness from islets isolated from wild-type mice that mimicked those previously reported (41). Wild-type islets exhibited a peak within 5 min of glucose stimulation, consistent with the occurrence of first phase insulin secretion. The first phase peak was followed by a sustained second phase that persisted at a level approximately 2-fold higher than basal level until glucose levels were reduced back to basal (2.8 mM). However, islets from Syn4 (−/+) mice showed a significant 50% reduction in first phase secretion (Fig. 4B), as quantitated by the area under the curve between 11 and 17 min. Second phase of secretion (18–45 min) from the Syn4 (−/+) islets showed a trend toward reduction in a compilation of three independent isolation and perifusion experiments, although this did not reach statistical significance. Furthermore, using an immunodepletion assay in Streptolysin-O permeabilized MIN6 cells, which is designed to assess secretion from the primed/docked pool (first phase) of insulin secretory granules and exclude secretion from mobilized granules, introduction of three independent sources of affinity-purified anti-Syn4 antibodies resulted in a 40–60% reduction in calcium-stimulated insulin secretion relative to IgG controls (data not shown). Thus, these data indicate that Syn4 was functionally essential for facilitating first-phase insulin secretion.

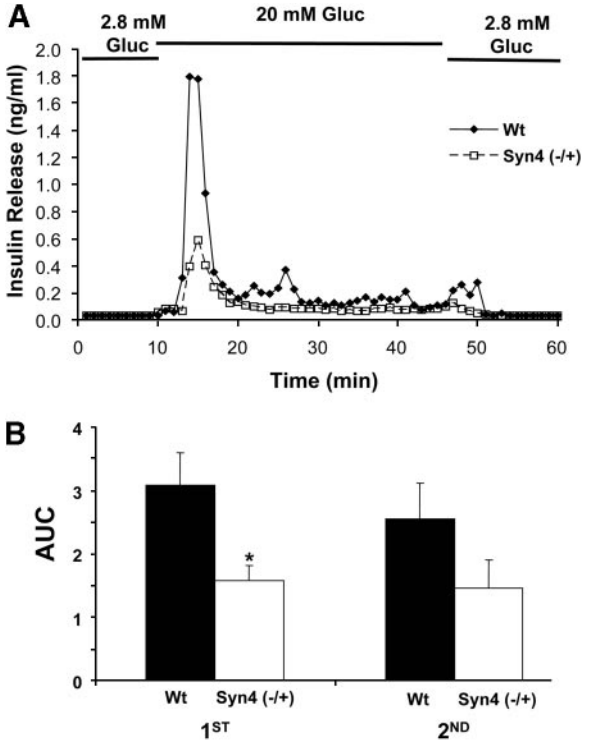

Fig. 4. Islets from Syn4 (−/+) Mice Have Significantly Impaired First Phase Insulin Secretion

Islets isolated from wild-type (Wt, *filled diamonds*) or Syn4 (−/+, *open squares*) mice were handpicked into groups of 50 and layered onto cytodex bead columns as described in *Materials and Methods*. A, Insulin release from a representative perifusion experiment. Islets were first preincubated for 30 min in low glucose (2.8 mM), then basal samples collected (1–10 min) at low glucose to establish baseline. Glucose was then elevated to 20 mM for 35 min, and subsequently returned to low glucose for 15 min. Eluted fractions were collected at 1-min intervals at a flow rate of 0.3 ml/min and insulin secretion determined by RIA. B, Quantitation of area under the curve (AUC) for first (11–17 min) and second (18–45 min) phase insulin secretion from islets isolated from Wt (*filled bars*) and Syn4 (−/+) mice (*open bars*), normalized to baseline. Data represent the average ± SE of three to five independent sets of islets. *, $P < 0.05$ *vs.* Wt islets.

To verify that the defect in glucose-stimulated insulin secretion resulted from specific reduction in Syn4 protein, we replenished Syn4 by adenoviral expression of recombinant protein in the Syn4 (−/+) islets and assessed biphasic insulin secretion (Fig. 5A). Freshly isolated Syn4 (−/+) islets were transduced [multiplicity of infection (M.O.I.) = 100] with adenoviral particles encoding enhanced green fluorescent protein (EGFP) (control, Con-Ad) or Syn4 protein (packaged with EGFP, Syn4-Ad) for 1 h followed by an overnight incubation. Islets exhibiting green fluorescence (infection efficiency ~90–100%) were handpicked into tubes for SDS-PAGE and immunoblotting analysis as performed in Fig. 1A. Syn4-Ad transduced islets showed 3.3-fold more Syn4 protein relative to Con-Ad transduced islets (Fig. 5, A and B). By contrast, Syn4 (−/+) islets transduced with either Con-Ad or Syn4-Ad showed equivalent abundances of Syn1, SNAP-25, and VAMP2. For analysis of biphasic secretion, green fluorescent islets were handpicked and placed onto dual columns and subjected to the identical perifusion regime described for Fig. 4. Syn4 (−/+) islets transduced with Syn4-Ad showed a full restoration of insulin secretion in each phase to levels observed in wild-type mice, whereas control transduced Syn4 (−/+) islets still showed deficient biphasic secretion (Fig. 5C). Quantitation of area under the curve revealed this to be a significant 40% increase in first phase secretion in islets transduced with Syn4-Ad compared with control transduced islets (Fig. 5D). Again, there was a trend for increased second phase secretion, although it did not reach statistical significance ($P = 0.08$). These data indicated that the abundance of Syn4 protein positively correlated with the level of insulin secreted during first phase insulin secretion.

Overexpression of Syntaxin 4 Enhances Insulin Secretion

Syn4 transgenic mice express approximately 3–5-fold more Syn4 protein in skeletal muscle, fat, pancreas, and the islets therefrom (24). These mice have in-

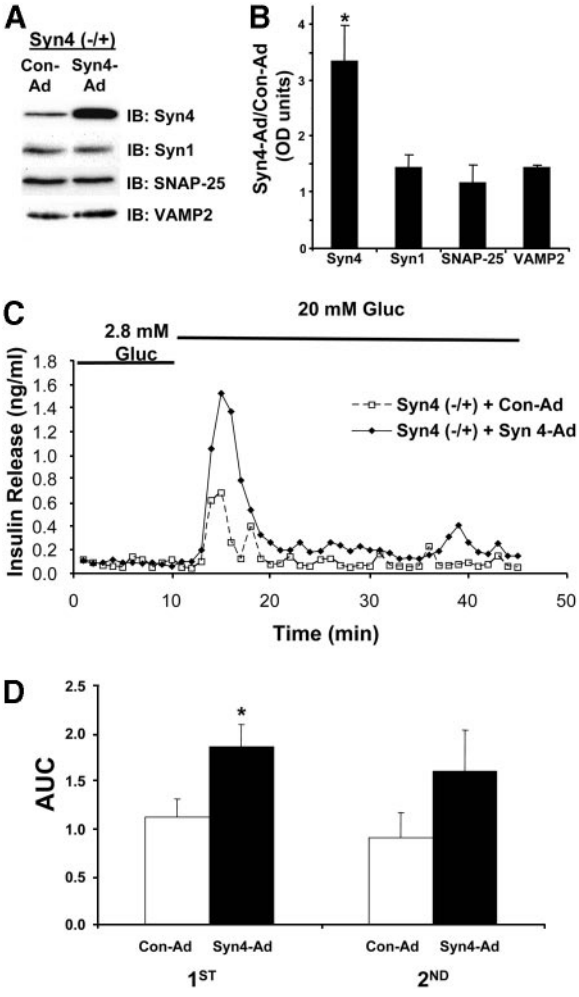

Fig. 5. Replenishment of Syn4 Protein Restores First Phase Insulin Secretion to Syn4 (−/+) Islets

Islets were isolated from Syn4 (−/+) mice and immediately transduced at M.O.I. = 100 with adenoviral particles encoding EGFP as control for infection (Con-Ad) or Syn4 (Syn4-Ad) for 1 h at 37 C. Islets were cultured overnight, after which green fluorescent labeled islets were handpicked under a fluorescence microscope for secretion studies. A, Approximately 200 Syn4 (−/+) islets transduced with Con-Ad or Syn4-Ad were solubilized in SDS-sample buffer and resolved on 12% SDS-PAGE, transferred to polyvinylidene difluoride and immunoblotted. B, OD scanning quantitation of three independent islet immunoblot experiments. Data were tabulated as the ratio of band density for Syn4-Ad relative to that of Con-Ad and are shown as means ± SE, *, $P < 0.05$ *vs.* Con-Ad. C, Insulin release from a representative sample of adenovirally transduced Syn4 (−/+) islets. Transduced islets (Con-Ad, *open squares*; Syn4-Ad, *filled diamonds*) were handpicked into groups of 50 and placed onto columns for perifusion analysis as described in Fig. 4. D, Quantitation of area under the curve (AUC) for first (11–17 min) and second (18–45 min) phase insulin secretion from islets transduced with Con-Ad (*open bars*) and Syn4-*Ad (filled bars*), normalized to baseline. Data represent the average ± SE of three to five independent sets of islets. *, $P < 0.05$ *vs.* Con-Ad islets; Gluc, D-glucose.

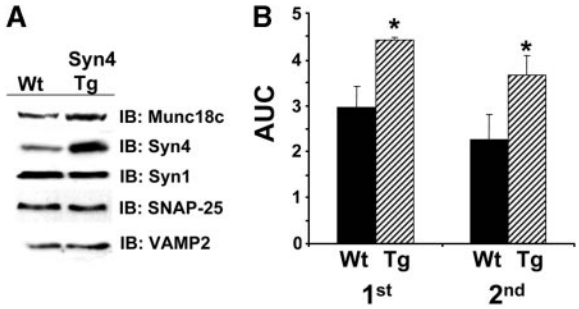

Fig. 6. Overexpression of Syn4 Confers Enhanced Biphasic Insulin Secretion

Islets were isolated from wild-type (Wt) or Syn4 Tg mice. A, Approximately 200 islets were solubilized in SDS-sample buffer and resolved on 12% SDS-PAGE, and transferred to polyvinylidene difluoride for immunoblotting. B, Islets were hand picked and placed on columns for perifusion as described in Fig. 4. First and second phase quantitation of area under the curve (AUC) for Wt (*filled bars*) and Syn4 Tg islets (*diagonal lined bars*) normalized to baseline. Data represent the average ± SE of four to six independent sets of islets. *, $P < 0.05$ *vs.* Wt islets.

creased insulin sensitivity and are protected against high-fat diet-induced insulin resistance (24, 42). The increased sensitivity was found to be resultant from an increased rate of glucose uptake mediated by increased GLUT4 translocation in skeletal muscle, due presumably to the increased number of Syn4-based fusion sites at the plasma membrane. Analogously, we questioned whether islets isolated from the Syn4 transgenic (Syn4 Tg) mice would show an increased amplitude or rate of first or second phase glucose-stimulated insulin secretion. As previously reported (24), Syn4 Tg islets contained 2.4-fold more Syn4 and 1.7-fold more Munc18c protein than wild-type islets, with no significant alterations in other exocytic proteins such as Syn1, SNAP-25, or VAMP2 (Fig. 6A). In perifusion experiments, Syn4 Tg islets displayed significant increases in amplitude of each phase insulin secretion compared with wild-type islets, and quantitation of area under the curve showed this to be a significant 35% increase in the extent of insulin release during each phase of secretion (Fig. 6B). Similarly, in glucose tolerance tests we observed that serum insulin levels of Syn4 Tg mice peaked within 5 min, compared with the 15–30 min required by Wt mice to reach the same peak ($P < 0.02$) (24). Islets taken from Syn4 Tg mice showed significantly enhanced quantities of insulin released in response to 20 mM glucose: Syn4 Tg was 5.36 ± 1.11, *vs.* Wt at 2.68 ± 0.36 pg/ml/10 islets normalized for insulin content ($P < 0.05$). Basal secretion was insignificantly increased in Syn4 Tg islets: 0.73 ± 0.29, *vs.* Wt: 0.33 ± 0.03 pg/ml/10 islets normalized for insulin content ($P = 0.16$). However, when expressed in terms of stimulation index (glucose-stimulated/basal secretion), Syn4 Tg islet secretion did not statistically differ from that of Wt islets (ranged from 11- to 14-fold for Syn4 Tg *vs.* 10- to 11-fold for Wt) (24). Taken together, these

data suggest that increased Syn4 and Munc18c may functionally accelerate insulin release *in vivo*.

DISCUSSION

In this report, we present the first evidence that Syn4 plays and essential positive role in the exocytosis of insulin granules. Islets isolated from Syn4 (−/+) knockout mice displayed a significant impairment in the first phase of glucose-stimulated insulin secretion, although exhibited basal secretion levels similar that of wild-type islets. Immunofluorescent confocal microscopy revealed that Syn4 was primarily localized to islet β-cells of the mouse islet, suggesting that Syn4 functioned directly in insulin granule exocytosis and not indirectly in another cell type of the islet. In MIN6 β-cells, siRNA-mediated reduction of Syn4 resulted in impaired glucose-stimulated insulin secretion, consistent with the islet data. Mechanistically, wild-type abundance of Syn4 was shown to be required for peak amplitude and extent of insulin release during both phases of secretion. This was demonstrated by the partial loss of function in Syn4 (−/+) islets, and by the complete restoration of function upon specific replenishment of Syn4-Ad to Syn4 (−/+) islets. Importantly, enhanced Syn4 abundance in Syn4 Tg islets conferred significantly enhanced insulin secretion during both phases. Altogether, these data are consistent with a model whereby Syn4-based complexes function as fusion sites for docked and primed granules released during first phase secretion, and that the addition of more Syn4 sites (as in the Syn4 Tg islets) can be accessed by granule pools during second phase secretion. Thus, the addition of more Syn4-based fusion sites at the plasma membrane could be advantageous in efforts to increase the number of granule fusion events occurring per phase, *in vivo*.

In 1996, Syn1 was identified as the critical t-SNARE responsible for mediating fusion of insulin secretory granules to the plasma membrane (13, 14, 43). Syn1 is known to be essential for calcium-stimulated insulin secretion (13). This is likely due to a direct interaction between Syn1 and the L_D-voltage-dependent Ca^{2+} channel in pancreatic β-cells (13). Calcium influx is known to facilitate the immediate fusion of insulin secretory granules located in the ready releasable pool with the plasma membrane. Therefore, it had been proposed that Syn1 regulates first phase insulin secretion. However, depletion of Syn1 resulted in only a 25% loss of glucose-stimulated insulin secretion (12, 44, 45), suggesting that a second VAMP2-based mechanism must exist to account for the deficit.

However, Syn4 (−/+) islets showed significantly diminished first-phase secretion in the perifusion analysis, with a trend toward reduction in second phase secretion as well. The requirement for a particular abundance of Syn4 was further confirmed by the restoration of function upon specific replenishment of Syn4 by adenoviral expression. Consistent with this, overexpression of Synip reduced glucose-stimulated insulin release during both phases, presumably by binding and sequestering endogenous Syn4 (18). However, alteration of abundance of Syn4 results in coordinate changes in Munc18c, such that it is theoretically possible that the phenotype of the Syn4 (−/+) islets is due to the loss of Syn4, Munc18c, or the Syn4-Munc18c complex. Further studies are needed to discriminate the requirement for Syn4 alone in the absence of alterations of Munc18c expression.

Whereas both Syn1 and Syn4 isoforms are required for insulin secretion, they do not appear to be used in an entirely redundant manner. Although each binds VAMP2 and SNAP-25 in MIN6 cells (data not shown), Syn1 complexes with Munc18–1, whereas Syn4 is specific for Munc18c (46–50). In addition, SNARE core complex formation featuring either Syn1 or Syn4 as its t-SNARE could be activated by different secretagogues, GTPases, or by differential localization at the plasma membrane. For example, we have shown that the cycling of the Rho family GTPase Cdc42 is activated specifically upon glucose induction, whereas GTPases Rac and Rap are stimulated via glucose or potassium stimulation (51–53). In addition, we and others have reported that Syn1 interacts with Cdc42 (33, 54), but that Syn4 does not (Thurmond, D. C., unpublished). Alternatively, Syn1 and Syn4 may be differentially localized to plasma membrane or caveolar lipid domains. In support of this, we have been able to coimmunoprecipitate Syn1 but not Syn4 with the caveolar marker protein Caveolin-1 (Nevins, A. K., and D. C. Thurmond, manuscript submitted) providing evidence that t-SNAREs are partitioned at the plasma membrane and this compartmentalization could be essential in triggering different events leading to biphasic insulin secretion. In addition, recent works have begun to elucidate the effects of certain glucose potentiators in partitioning granules into distinct pools for release (55). Use of these glucose potentiators such as free fatty acids, GLP-1 or carbachol with the Syn4 (−/+) islets will aid in the determination of the role of Syn4 in granule exocytosis from the readily- and immediate releasable pools and/or in mobilization of granules from the storage pools, and will also contribute to defining a specific role for Syn4 relative to Syn1 in biphasic insulin granule exocytosis.

Perifusion analysis of the Syn4 Tg islets indicated that overexpression of Syn4 protein coincided with significant increase of glucose-stimulated insulin secretion during both phases. Because biphasic secretion in the Syn4 Tg islets occurred during the same time periods (10–17 min) but showed increased peak amplitude, the data support the notion that the additional Syn4 provided more insulin granule fusion sites that were utilizable by the various pools of granules, culminating in a faster rate of fusion. Conversely, Syn1 overexpression in cultured cells and in islets causes inhibition of insulin secretion (18, 56), suggesting that the mechanistic details underlying Syn1 *vs.* Syn4-regulated fusion might differ. In fact,

overexpression of Syn1 inhibited L-type calcium channel activity, insulin biosynthesis and exocytosis in β-cell lines, whereas overexpression of Syn4 was without effect (57). The difference of effects of overexpression between Syn1 and Syn4 may lie in their potential to bind and sequester cellular proteins essential to exocytosis, *e.g.* Syn1 binds to the L-type calcium channel, potassium channels, Cdc42, and Caveolin-1. Therefore, increased amounts of Syn4 but not Syn1 were beneficial to augmentation of insulin secretion, and further elucidation of the signaling pathway(s) leading to Syn4-based complexes may provide new targets for pharmacological intervention.

The Syn4 (−/+) mice are characterized as insulin resistant and glucose intolerant at 4–6 months of age (27). The insulin resistance correlated with a defect in whole body and skeletal muscle glucose uptake, attributed to reduced insulin-stimulated GLUT4 vesicle fusion with the plasma membrane. However, in the present studies the islets used were collected from 8- to 12-wk-old mice, and at this age the Syn4 (−/+) knockout mice were still glucose tolerant (data not shown). Thus, these defects in insulin secretion clearly preceded the onset of peripheral insulin resistance. Although further experiments will be required to establish the role of Syn4 in biphasic insulin secretion, our data are consistent with the concept that reductions in insulin release may precede insulin resistance and represent a primary genetic risk factor predisposing individuals to type 2 diabetes (58). In some cases, the loss of first-phase insulin secretion is known to occur in type 2 diabetic patients, and rodent models of insulin resistance and type 2 diabetes have been reported to have aberrant expression of SNARE proteins including Syn4 and Syn1 (27, 59) However, whether there is a correlation between aberrant Syn4 or Syn1 levels and type 2 diabetes in humans must await further investigation.

In summary, this is the first report documenting an essential role for Syn4 in glucose-stimulated insulin secretion in isolated mouse islets and pancreatic β-cells. Moreover, we demonstrate that increased expression of Syn4 in islets generated β-cells with increased capacity to secrete insulin in a regulated and biphasic manner. Further research will focus on defining pathway(s) leading to Syn4-based fusion complexes as well as distinguishing the mechanisms underlying Syn1-based granule fusion from Syn4-based granule fusion in biphasic insulin secretion.

MATERIALS AND METHODS

Materials

The rabbit polyclonal Syntaxin 4 and VAMP2 antibodies were obtained through Chemicon (Temecula, CA) and SYSY (Gottingen, Germany), respectively. Syntaxin 1 and clathrin antibodies were purchased from Upstate Biotechnology (Lake Placid, NY) and Transduction Laboratories (Lexington, KY), respectively. Goat antirabbit-horseradish peroxidase and antimouse-horseradish peroxidase secondary antibodies and Tfx-50 lipofection reagent were acquired from Bio-Rad (Hercules, CA). The RIA grade BSA, Streptolysin-O and D-glucose were obtained from Sigma (St. Louis, MO). MIN6 cells were a gift from Dr. John Hutton (University of Colorado Health Sciences Center, Denver, CO). Hyperfilm-MP and enhanced chemiluminescence (ECL) reagent were obtained from Amersham Biosciences (Piscataway, NJ). Supersignal Ultra ECL reagent and Vectashield were purchased from Pierce (Rockford, IL) and Vector Laboratories (Burlingame, CA), respectively. Texas Red, fluorescein isothiocyanate (FITC), and Cy5-conjugated secondary antibodies were purchased from Jackson ImmunoResearch Laboratories (West Grove, PA). The human C-peptide, rat insulin, and sensitive rat insulin RIA kits were acquired from Linco Research Inc. (St. Charles, MO). All other chemicals were of reagent grade or best quality commercially available.

Plasmids

The pSilencer1.0-Syn4 construct no. 3 (siSyn4) was generated by insertion of annealed complimentary double-stranded oligonucleotides encoding 19 nucleotides (nt) (TGCAGTCCGAATACCGAGA) of rat Syntaxin 4, followed by a loop region (TTCAAGAGA) and the antisense of the 19 nt. The pSilencer1.0 control construct (siCon) was generated similarly, using a 19-nt sequence (GCGCGCTTTGTAGGATTCG) that failed to recognize any other mammalian protein using the basic local assignment and search tool (36). Similarly, siRNAs encoding Syn4 nos. 1, 2, and 4 were as follows: no. 1, GTTCGGCAGACTATGGCCAA; no. 2, GCCTGCGAGAGGAGATCAAA; no. 4, GCCGCATCGAGAAGAACATC. Oligonucleotides were generated to encode *Apa*I and *Eco*RI sites at the 5′ and 3′ ends for insertion into the pSilencer 1.0 vector (Ambion, Inc.). The Syn4-Ad adenovirus was generated by insertion of the full-length rat Syntaxin 4 cDNA into the 5′ *Eco*RI site and the 3′ *Xba*I site of the pAdTREpA vector (Dr. Beverly Davis, University of Iowa Gene Transfer Vector Core, Iowa City, IA). The construct was linearized by restriction digestion with *Xba*I and packaged with EGFP to enable visualization of infection efficiency. pAdCMV-EGFP (Con-Ad) purchased from The University of Iowa Gene Transfer Vector Core Facility and used as a control for adenoviral infection. Both adenoviruses were generated from single plaques.

Cell Culture, Transient Transfection, and Insulin Secretion

CHO-K1 cells were purchased from the American Type Culture Collection (Manassas, VA) and cultured in Ham's F-12 medium supplemented with 10% fetal bovine serum, 100 U/ml penicillin, 100 μg/ml streptomycin and 292 μg/ml L-glutamine. At 80–90% confluence, cells were electroporated with 40 μg DNA as previously described (34), thus obtaining approximately 70% of cells transfected. After 48 h incubation, cells were harvested in Nonidet P-40 lysis buffer (1% Nonidet P-40, 10% glycerol, 50 μM sodium fluoride, 10 mM sodium pyrophosphate, 1 mM sodium vanadate, 137 mM sodium chloride, 1 mM phenylmethylsulfonyl fluoride, 1 μg/ml pepstatin, 10 μg/ml aprotinin, and 5 μg/ml leupeptin) and lysates cleared after microcentrifugation for 10 min at 4 C for subsequent immunoblotting. MIN6 cells were cultured in DMEM (25 mM glucose) supplemented with 15% fetal bovine serum, 100 U/ml penicillin, 100 μg/ml streptomycin, and 292 μg/ml L-glutamine and 50 μM β-mercaptoethanol as described previously (33, 60–62). At 40–50% confluence, cells were cotransfected with 2.5 μg of each plasmid DNA and human proinsulin (pCB6/INS, a gift from Dr. Chris Newgard, Duke University, Durham, NC) as previously described (18). After 48 h incubation, cells were washed twice and incubated for 2 h in MKRBB [5 mM KCl, 120 mM NaCl, 15 mM HEPES (pH 7.4), 24 mM $NaHCO_3$, 1 mM $MgCl_2$, 2 mM $CaCl_2$, and 0.1% BSA], stimulated with 20 mM glucose for 1 h and supernatant collected for quantitation using a human C-peptide immunoassay kit (Linco Research, Inc.).

Subcellular Fractionation

Subcellular fractions were isolated as previously described (33). Briefly, MIN6 cells at 70–80% confluence were washed with cold PBS and harvested into 1 ml of homogenization buffer [20 mM Tris-HCl (pH 7.4), 0.5 mM EDTA, 0.5 mM EGTA, 250 mM sucrose, and 1 mM dithiothreitol containing the following protease inhibitors: leupeptin (10 μg/ml), aprotinin (4 μg/ml), pepstatin (2 μg/ml), and phenylmethylsulfonyl fluoride (100 μM)]. Cells were disrupted by 10 strokes through a 27-gauge needle and homogenates centrifuged at 900 $\times$ *g* for 10 min. Postnuclear supernatants were centrifuged at 5500 $\times$ *g* for 15 min and the subsequent supernatant centrifuged at 25,000 $\times$ *g* for 20 min to obtain the secretory granule fraction in the pellet. The supernatant was further centrifuged at 100,000 $\times$ *g* for 1 h to obtain the cytosolic fraction. All steps were performed at 4 C. Plasma membrane fractions were obtained by mixing the postnuclear pellet with 1 ml Buffer A (0.25 M sucrose, 1 mM $MgCl_2$, and 10 mM Tris-HCl (pH 7.4)] and 2 vol Buffer B [2 M sucrose, 1 mM $MgCl_2$, and 10 mM Tris-HCl (pH 7.4)]. The mixture was overlaid with Buffer A and centrifuged at 113,000 $\times$ *g* for 1 h to obtain an interface containing the plasma membrane. The interface was collected and diluted to 2 ml with homogenization buffer for centrifugation at 3000 $\times$ *g* for 10 min, and the resulting pellet collected as the plasma membrane fraction.

Mice

All studies involving mice followed the guidelines for the use and care of laboratory animals. Syntaxin 4 heterozygous (−/+) knockout mice were the kind gift of Jeffrey Pessin (SUNY, Stonybrook, NY) and express 50% less Syntaxin 4 protein in all major tissues and organs (27). Syn4 (−/+) mice used in these studies were bred in the Laboratory Animal Resource Center facility at the Indiana University School of Medicine for at least six generations to C57BL/6J strain mice, bringing the background enrichment to at least F10. Syntaxin 4 transgenic (Syn4 Tg) mice were generated as described previously (24), with founder mice of the C57BL/6J background strain. Syn4 is expressed at 3- to 5-fold over that of endogenous in skeletal muscle, adipose tissue, and pancreas tissues only (24).

Isolation and Culture of Mouse Islets

Pancreatic mouse islets were isolated as previously described (19) as adapted from Lacy (63). Briefly, pancreata from 8- to 12-wk-old male mice were digested with collagenase and purified using a Ficoll density gradient. After isolation, islets were cultured overnight at 37 C/ 5% CO_2 in CMRL-1066 media (static and perifusion experiments) or RPMI-1640 (for adenoviral infection).

Immunofluorescence and Confocal Microscopy

Islets were isolated from wild-type mice, washed with PBS, handpicked onto glass coverslips, and affixed with Cell-Tak (BD Biosciences, Bedford MA). Islets were immediately fixed in 4% paraformaldehyde for 25 min and permeabilized in 3% Triton X-100 for 3–4 h at room temperature. Fixed islets were blocked in 5% donkey serum (Sigma, St. Louis, MO) in 0.15% Triton X-100 overnight at 4 C. Islets were equilibrated at room temperature in antibody incubation buffer (0.2% Triton X-100/1% BSA/PBS) for 20 min, followed by an overnight incubation with mouse antiinsulin and guinea pig antiglucagon (1:1000) and rabbit anti-Syntaxin 4 (1:500) reconstituted in antibody incubation buffer at 4 C. Islets were then washed three times with 0.2% Triton X-100/1% BSA/PBS for 30 min at room temperature, followed by incubation with anti-Texas Red, FITC or Cy5 secondary antibodies (1:1000) overnight at 4 C. Islets were then washed three times in PBS, overlayed with vectashield mounting medium and coverslips mounted for imaging analysis using the Zeiss 510 confocal microscope (Carl Zeiss, Jena, Germany).

Static Culture

Fresh islets from wild-type and Syntaxin 4 heterozygous (−/+) mice were hand-picked into groups of 10, preincubated in KRBH [10 mM HEPES (pH 7.4), 134 mM NaCl, 5 mM $NaHCO_3$, 4.8 mM KCl, 1 mM $CaCl_2$, 1.2 mM $MgSO_4$, 1.2 mM KH_2PO_4] containing 2.8 mM glucose and 0.1% BSA for 2 h, followed by stimulation with 20 mM glucose for 2 h. Media were collected to measure insulin secretion and islets were harvested in Nonidet P-40 lysis buffer as described above to determine cellular insulin content by RIA.

Perifusion of Islets

Islets were handpicked into groups of 50 onto a column between two layers of Cytodex 3 beads (Amersham Biosciences, Piscataway, NJ), washed twice with Dulbecco's PBS (magnesium-free) and preincubated for 30 min at 37 C in KRBH as described above. Islets were perifused at a flow rate of 0.3 ml/min for 10 min in KRBH containing 2.8 mM glucose with eluted fractions captured at 1-min intervals, followed by glucose stimulation (20 mM) for 35 min. Insulin secreted into eluted fractions was quantitated by a sensitive rat insulin RIA (Linco Research, Inc.).

Adenoviral Transduction of Islets

Islets were isolated as described above, and immediately transduced at an M.O.I. = 100 with either Syn4-Ad or Con-Ad CsCl-purified particles titered at 1×10^{10} pfu/ml and 3×10^{10} pfu/ml, respectively, for 1 h at 37 C. Transduced islets were then washed twice and incubated overnight in RPMI-1640 at 37 C/5% CO_2. EGFP fluorescence was visualized in greater than 95% of cells in all experiments. EGFP fluorescent islets were handpicked for perifusion analysis.

Statistical Analysis

All data expressed as mean ± SE. Data were evaluated for statistical significance using Student's *t* test.

Acknowledgments

We are very grateful to Drs. Chris Newgard (Duke University, Durham, NC), Richard Scheller (Stanford University, Stanford, CA), John Hutton (UCHSC, Denver, CO), and Jeffrey Pessin (SUNY, Stonybrook, NY) for gifts of human proinsulin cDNA, Syntaxin 4 cDNA, MIN6 cells, and mice, respectively. We thank Dr. Keith Tornheim (Boston University, Boston, MA) for his expertise and advice on the islet perifusion experiments. We would also like to thank Angela Nevins for technical assistance and critical review of the manuscript.

Received April 18, 2005. Accepted August 4, 2005.

Address all correspondence and requests for reprints to: Debbie C. Thurmond, Ph.D., Department of Biochemistry & Molecular Biology, Center for Diabetes Research, Indiana University School of Medicine, Indianapolis, Indiana 46202. E-mail: dthurmon@iupui.edu.

This study was supported by grants from the American Diabetes Association (1-03-CD-10), the National Institutes of Health (DK-067912) and the Indiana University School of Medicine Showalter Trust (D.C.T.). B.A.S. was supported by

a Diabetes Graduate Student fellowship from Indiana University School of Medicine.

REFERENCES

1. Straub SG, Sharp GW 2002 Glucose-stimulated signaling pathways in biphasic insulin secretion. Diabetes Metab Res Rev 18:451–463
2. Rorsman P, Eliasson L, Renstrom E, Gromada J, Barg S, Gopel S 2000 The cell physiology of biphasic insulin secretion. News Physiol Sci 15:72–77
3. Bratanova-Tochkova TK, Cheng H, Daniel S, Gunawardana S, Liu Y-J, Mulvaney-Musa J, Schermerhorn T, Straub SG, Yajima H, Sharp GWG 2002 Triggering and augmentation mechanisms, granule pools, and biphasic insulin secretion. Diabetes 51:S83–S90
4. Olofsson CS, Gopel SO, Barg S, Galvanovskis J, Ma X, Salehi A, Rorsman P, Eliasson L 2002 Fast insulin secretion reflects exocytosis of docked granules in mouse pancreatic B-cells. Pflugers Arch 444:43–51
5. Barg S, Eliasson L, Renstrom E, Rorsman P 2002 A subset of 50 secretory granules in close contact with L-type Ca2+ channels accounts for first-phase insulin secretion in mouse β-cells. Diabetes 51:S74–S82
6. Straub SG, Sharp GWG 2004 Hypothesis: one rate-limiting step controls the magnitude of both phases of glucose-stimulated insulin secretion. Am J Physiol Cell Physiol 287:C565–C571
7. Nesher R, Cerasi E 2002 Modeling phasic insulin release: immediate and time-dependent effects of glucose. Diabetes 51:S53–S59
8. Sadoul K, Lang J, Montecucco C, Weller U, Regazzi R, Catsicas S, Wollheim CB, Halban PA 1995 SNAP-25 is expressed in islets of Langerhans and is involved in insulin release. J Cell Biol 128:1019–1028
9. Lang J 1999 Molecular mechanisms and regulation of insulin exocytosis as a paradigm of endocrine secretion. Eur J Biochem 259:3–17
10. Lin RC, Scheller RH 2000 Mechanisms of synaptic vesicle exocytosis. Ann Rev Cell Dev Biol 16:19–49
11. Regazzi R, Wollheim CB, Lang J, Theler JM, Rossetto O, Montecucco C, Sadoul K, Weller U, Palmer M, Thorens B 1995 VAMP-2 and cellubrevin are expressed in pancreatic β-cells and are essential for Ca^{2+}-but not for GTPγ S-induced insulin secretion. EMBO J 14:2723–2730
12. Lang J, Zhang H, Vaidyanathan VV, Sadoul K, Niemann H, Wollheim CB 1997 Transient expression of botulinum neurotoxin C1 light chain differentially inhibits calcium and glucose induced insulin secretion in clonal β-cells. FEBS Lett 419:13–17
13. Yang SN, Larsson O, Branstrom R, Bertorello AM, Leibiger B, Leibiger IB, Moede T, Kohler M, Meister B, Berggren PO 1999 Syntaxin 1 interacts with the L(D) subtype of voltage-gated Ca^{2+} channels in pancreatic β cells. Proc Natl Acad Sci USA 96:10164–10169
14. Jacobsson G, Bean AJ, Scheller RH, Juntti-Berggren L, Deeney JT, Berggren PO, Meister B 1994 Identification of synaptic proteins and their isoform mRNAs in compartments of pancreatic endocrine cells. Proc Natl Acad Sci USA 91:12487–12491
15. Wheeler MB, Sheu L, Ghai M, Bouquillon A, Grondin G, Weller U, Beaudoin AR, Bennett MK, Trimble WS, Gaisano HY 1996 Characterization of SNARE protein expression in β cell lines and pancreatic islets. Endocrinology 137:1340–1348
16. Chen YA, Scheller RH 2001 SNARE-mediated membrane fusion. Nat Rev Mol Cell Biol 2:98–106
17. Oh E, Spurlin BA, Pessin JE, Thurmond DC 2005 Munc18c heterozygous knockout mice display increased susceptibility for severe glucose intolerance. Diabetes 54:638–647
18. Saito T, Okada S, Yamada E, Ohshima K, Shimizu H, Shimomura K, Sato M, Pessin JE, Mori M 2003 Syntaxin 4 and Synip (syntaxin 4 interacting protein) regulate insulin secretion in the pancreatic β HC-9 cell. J Biol Chem 278:36718–36725
19. Spurlin BA, Thomas RM, Nevins AK, Kim H-J, Kim Y-J, Noh H-L, Shulman GI, Kim JK, Thurmond DC 2003 Insulin resistance in tetracycline-repressible Munc18c transgenic mice. Diabetes 52:1910–1917
20. Olson AL, Knight JB, Pessin JE 1997 Syntaxin 4, VAMP2, and/or VAMP3/cellubrevin are functional target membrane and vesicle SNAP receptors for insulin-stimulated GLUT4 translocation in adipocytes. Mol Cell Biol 17:2425–2435
21. Volchuk A, Wang Q, Ewart HS, Liu Z, He L, Bennett MK, Klip A 1996 Syntaxin 4 in 3T3–L1 adipocytes: regulation by insulin and participation in insulin-dependent glucose transport. Mol Biol Cell 7:1075–1082
22. Rea S, Martin LB, McIntosh S, Macaulay SL, Ramsdale T, Baldini G, James DE 1998 Syndet, an adipocyte target SNARE involved in the insulin-induced translocation of GLUT4 to the cell surface. J Biol Chem 273:18784–18792
23. Araki S, Tamori Y, Kawanishi M, Shinoda H, Masugi J, Mori H, Niki T, Okazawa H, Kubota T, Kasuga M 1997 Inhibition of the binding of SNAP-23 to syntaxin 4 by Munc18c. Biochem Biophys Res Commun 234:257–262
24. Spurlin BA, Park SY, Nevins AK, Kim JK, Thurmond DC 2004 Syntaxin 4 transgenic mice exhibit enhanced insulin-mediated glucose uptake in skeletal muscle. Diabetes 53:2223–2231
25. Thurmond DC, Pessin JE 2001 Molecular machinery involved in the insulin-regulated fusion of GLUT4-containing vesicles with the plasma membrane. Mol Membr Biol 18:237–245
26. Olson AL, Pessin JE 1996 Structure, function and regulation of the mammalian facilitative glucose transporter gene family. Ann Rev Nutr 16:235–256
27. Yang C, Coker KJ, Kim JK, Mora S, Thurmond DC, Davis AC, Yang B, Williamson RA, Shulman GI, Pessin JE 2001 Syntaxin 4 heterozygous knockout mice develop muscle insulin resistance. J Clin Invest 107:1311–1318
28. Rowe J, Corradi N, Malosio ML, Taverna E, Halban P, Meldolesi J, Rosa P 1999 Blockade of membrane transport and disassembly of the Golgi complex by expression of syntaxin 1A in neurosecretion-incompetent cells: prevention by rbSEC1. J Cell Sci 112:1865–1877
29. Kowluru A, Seavey SE, Rhodes CJ, Metz SA 1996 A novel regulatory mechanism for trimeric GTP-binding proteins in the membrane and secretory granule fractions of human and rodent β cells. Biochem J 313:97–107
30. Pevsner J, Hsu SC, Braun JE, Calakos N, Ting AE, Bennett MK, Scheller RH 1994 Specificity and regulation of a synaptic vesicle docking complex. Neuron 13:353–361
31. Wasmeier C, Hutton JC 1996 Molecular cloning of phogrin, a protein-tyrosine phosphatase homologue localized to insulin secretory granule membranes. J Biol Chem 271:18161–18170
32. Baumert M, Mollard GFV, Jahn R, Sudhof TC 1989 Synaptobrevin: an integral membrane protein of 18,000 daltons present in small synaptic vesicles of rat brain. EMBO J 8:379–384
33. Nevins AK, Thurmond DC 2005 A direct interaction between Cdc42 and vesicle-associated membrane protein 2 regulates SNARE-dependent insulin exocytosis. J Biol Chem 280:1944–1952
34. Thurmond DC, Ceresa BP, Okada S, Elmendorf JS, Coker K, Pessin JE 1998 Regulation of insulin-stimulated GLUT4 translocation by Munc18c in 3T3L1 adipocytes. J Biol Chem 273:33876–33883
35. Schiavo G, Shone CC, Bennett MK, Scheller RH, Montecucco C 1995 Botulinum neurotoxin type C cleaves a single Lys-Ala bond within the carboxyl-terminal region of syntaxins. J Biol Chem 270:10566–10570

36. Gonzalez E, Nagiel A, Lin AJ, Golan DE, Michel T 2004 Small interfering RNA-mediated down-regulation of caveolin-1 differentially modulates signaling pathways in endothelial cells. J Biol Chem 279:40659–40669
37. Kashima Y, Miki T, Shibasaki T, Ozaki N, Miyazaki M, Yano H, Seino S 2001 Critical role of cAMP-GEFII-Rim2 complex in incretin-potentiated insulin secretion. J Biol Chem 276:46046–46053
38. Mulder H, Lu D, Finley J, IV, An J, Cohen J, Antinozzi PA, McGarry JD, Newgard CB 2001 Overexpression of a modified human malonyl-CoA decarboxylase blocks the glucose-induced increase in malonyl-CoA level but has no impact on insulin secretion in INS-1-derived (832/13) β-cells. J Biol Chem 276:6479–6484
39. Beguin P, Nagashima K, Gonoi T, Shibasaki T, Takahashi K, Kashima Y, Ozaki N, Geering K, Iwanaga T, Seino S 2001 Regulation of Ca^{2+} channel expression at the cell surface by the small G-protein kir/Gem. Nature 411:701–706
40. Ozaki N, Shibasaki T, Kashima Y, Miki T, Takahashi K, Ueno H, Sunaga Y, Yano H, Matsuura Y, Iwanaga T, Takai Y, Seino S 2000 cAMP-GEFII is a direct target of cAMP in regulated exocytosis. Nat Cell Biol 2:805–811
41. Preitner F, Ibberson M, Franklin I, Binnert C, Pende M, Gjinovci A, Hansotia T, Drucker DJ, Wollheim C, Burcelin R, Thorens B 2004 Gluco-incretins control insulin secretion at multiple levels as revealed in mice lacking GLP-1 and GIP receptors. J Clin Invest 113:635–645
42. Cho YR, Park, SY, Spurlin, BA, Kim, HJ, Higashimori, T, Kim, YG, Lee, MK, Thurmond, DC, Kim, JK 2004 Transgenic mice with overexpression of syntaxin 4 are protected from diet-induced insulin resistance in peripheral tissues. Diabetes 53:A71–A72
43. Daniel S, Noda M, Straub SG, Sharp GW, Komatsu M, Schermerhorn T, Aizawa T 1999 Identification of the docked granule pool responsible for the first phase of glucose-stimulated insulin secretion. Diabetes 48:1686–1690
44. Martin F, Salinas E, Vazquez J, Soria B, Reig JA 1996 Inhibition of insulin release by synthetic peptides shows that the H3 region at the C-terminal domain of syntaxin-1 is crucial for Ca(2+)- but not for guanosine 5′-[γ-thio] triphosphate-induced secretion. Biochem J 320:201–205
45. Martin F, Moya F, Gutierrez LM, Reig JA, Soria B 1995 Role of syntaxin in mouse pancreatic β cells. Diabetologia 38:860–863
46. Thurmond DC, Kanzaki M, Khan AH, Pessin JE 2000 Munc18c function is required for insulin-stimulated plasma membrane fusion of GLUT4 and insulin-responsive amino peptidase storage vesicles. Mol Cell Biol 20:379–388
47. Tellam JT, McIntosh S, James DE 1995 Molecular identification of two novel Munc-18 isoforms expressed in non-neuronal tissues. J Biol Chem 270:5857–5863
48. Tellam JT, Macaulay SL, McIntosh S, Hewish DR, Ward CW, James DE 1997 Characterization of Munc-18c and syntaxin-4 in 3T3–L1 adipocytes. Putative role in insulin-dependent movement of GLUT-4. J Biol Chem 272:6179–6186
49. Pevsner J, Hsu SC, Scheller RH 1994 n-Sec1: a neural-specific syntaxin-binding protein. Proc Natl Acad Sci USA 91:1445–449
50. Fujita Y, Sasaki T, Fukui K, Kotani H, Kimura T, Hata Y, Sudhof TC, Scheller RH, Takai Y 1996 Phosphorylation of Munc-18/n-Sec1/rbSec1 by protein kinase C. J Biol Chem 271:7265–7268
51. Kowluru A, Li G, Rabaglia ME, Segu VB, Hofmann F, Aktories K, Metz SA 1997 Evidence for differential roles of the Rho subfamily of GTP-binding proteins in glucose- and calcium-induced insulin secretion from pancreatic β cells. Biochem Pharmacol 54:1097–1108
52. Kowluru A, Seavey SE, Li G, Sorenson RL, Weinhaus AJ, Nesher R, Rabaglia ME, Vadakekalam J, Metz SA 1996 Glucose- and GTP-dependent stimulation of the carboxyl methylation of CDC42 in rodent and human pancreatic islets and pure β cells. Evidence for an essential role of GTP-binding proteins in nutrient-induced insulin secretion. J Clin Invest 98:540–555
53. Straub SG, Shanmugam G, Sharp GWG 2004 Stimulation of insulin release by glucose is associated with an increase in the number of docked granules in the β-cells of rat pancreatic islets. Diabetes 53:3179–3183
54. Daniel S, Noda M, Cerione RA, Sharp GW 2002 A link between Cdc42 and syntaxin is involved in mastoparan-stimulated insulin release. Biochemistry 41:9663–9671
55. Gromada J, Rorsman, P 2004 New insights into the regulation of glucagon secretion by glucagon-like peptide-1. Horm Metab Res 36:822–829
56. Lam P, Leung L, Pasyk E, Sheu L, Tsushima RG, Osborne L, Gaisano HY 2005 Transgenic mice over-expressing syntaxin-1A as a diabetes mouse model. Diabetes 54:2744–2754
57. Kang Y, Huang X, Pasyk EA, Ji J, Holz GG, Wheeler MB, Tsushima RG, Gaisano HY 2002 Syntaxin-3 and syntaxin-1A inhibit L-type calcium channel activity, insulin biosynthesis and exocytosis in β-cell lines. Diabetologia 45:231–241
58. Gerich JE 2002 Is reduced first-phase insulin release the earliest detectable abnormality in individuals destined to develop type 2 diabetes? Diabetes 51:S117–S121
59. Nagamatsu S, Nakamichi Y, Yamamura C, Matsushima S, Watanabe T, Ozawa S, Furukawa H, Ishida H 1999 Decreased expression of t-SNARE, syntaxin 1, and SNAP-25 in pancreatic β-cells is involved in impaired insulin secretion from diabetic GK rat islets: restoration of decreased t-SNARE proteins improves impaired insulin secretion. Diabetes 48:2367–2373
60. Thurmond DC, Gonelle-Gispert C, Furukawa M, Halban PA, Pessin JE 2003 Glucose-stimulated insulin secretion is coupled to the interaction of actin with the t-SNARE (target membrane soluble N-ethylmaleimide-sensitive factor attachment protein receptor protein) complex. Mol Endocrinol 17:732–742
61. Nevins AK, Thurmond DC 2003 Glucose regulates the cortical actin network through modulation of Cdc42 cycling to stimulate insulin secretion. Am J Physiol Cell Physiol 285:C698–C710
62. Wasmeier C, Hutton JC 2001 Secretagogue-dependent phosphorylation of the insulin granule membrane protein phogrin is mediated by cAMP-dependent protein kinase. J Biol Chem 276:31919–31928
63. Lacy PE, Kostianovsky M 1967 Method for the isolation of intact islets of Langerhans from the rat pancreas. Diabetes 16:35–39

Molecular Endocrinology **is published monthly by The Endocrine Society (http://www.endo-society.org), the foremost professional society serving the endocrine community.**